DESIGN AND CALIBRATION OF OPTICAL TWEEZERS FOR SINGLE-MOLECULE STUDIES

A Thesis

Presented to the Faculty of the Graduate School

of Cornell University

in Partial Fulfillment of the Requirements for the Degree of

Master of Science

by

Richard Cheng-I Yeh

January 2002

ABSTRACT

Feedback-controlled optical tweezers are used to manipulate single biological molecules in experiments on deoxyribonucleic acid (DNA) substrates. Before we trust these measurements, it is essential to know the accuracy and the precision of the device. This thesis describes the design and calibration of the optical tweezers. We measure relative displacements with nanometer accuracy and forces with an accuracy of 10%. The chief source of imprecision is in the human positioning of the sample under study. The capability of the instrument is demonstrated by stretching single molecules of DNA because of the elasticity of DNA has previously been well characterized. This thesis also compares DNA elasticity measurements made on this device with previously published data. I demonstrate that this instrument is well suited for characterizing DNA molecules that are long (~ 4000 bp), but not for DNA that are relatively short (~ 1000 bp). Fit parameters for new DNA tethers containing 4400 base pairs (bp) of DNA agree with expected values. The optical tweezers instrument is accurate enough to determine that one-hour-old 4400-bp DNA tethers have degraded, losing some 4% of their length. Our current methods are not appropriate for measurements of force-extension of short DNA molecules, such as 1155-bp DNA tethers.

BIOGRAPHICAL SKETCH

Richard C. Yeh graduated from the California Institute of Technology in June 1998 with the degree of Bachelor of Science. He matriculated as a graduate student at Cornell University in August 1998.

ACKNOWLEDGMENTS

I thank Benjamin C. Jantzen, Steven J. Koch, Dr. Arthur La Porta, Alla Shundrovsky, and Professor Michelle D. Wang for continuous support, encouragement, and critical reading of this master's thesis. This work was supported by NIH Molecular Biophysics Training Grant T32 GM08267 and other grants from the NIH and from the Keck Foundation.

TABLE OF CONTENTS

LIST OF TABLES

LIST OF FIGURES

LIST OF ABBREVIATIONS

AOD	acousto-optic deflector
bp	base pairs
CCD	charge-coupled device
dc	direct current
DNA	deoxyribonucleic acid
dsDNA	double-stranded deoxyribonucleic acid
RNA	ribonucleic acid
RNAP	ribonucleic acid polymerase
ssDNA	single-stranded deoxyribonucleic acid

1. INTRODUCTION

Careful design and calibration of optical tweezers (optical trap) are essential to single molecule measurements, some of examples of which are shown in Figure 1. For example, in Figure 1A, we would like to study how RNA polymerase (RNAP) moves along its DNA template. This is achieved by attaching the RNAP to the surface of a microscope cover glass and attaching one end of the DNA to a bead or microsphere, which is held an optical trap. The motions of RNA polymerase are monitored via the bead. In order to convert the bead position into RNAP position along its template, we must know accurately and precisely the force and displacement of the bead as well as the elastic properties of the DNA between the RNAP and the bead. This thesis is thus composed of two sections: the design and calibration of the optical trap; and the calibration of the elasticity of the DNA by stretching single molecules of DNA.

Figure 1 Length and force measurements are needed to obtain quantitative results in three current experiments in the Wang laboratory. (A) Observation of DNA-dependent mRNA transcription: an RNA polymerase enzyme translocates a DNA molecule (Wang et al., 1998) much in the same way that a person flying a kite would pull the string. We want to study the enzyme's behavior at various features along the DNA molecule. **(B) Disruption of nucleosomes:** DNA is uncoiled from oppositely charged proteins by the application of longitudinal tension (Brower-Toland et al., 2002). We want to calculate the amount of DNA liberated during each uncoiling event. **(C) Unzipping of double-stranded DNA:** The amount of force necessary to separate the two helical strands depends on the sequence of bases at the separation fork (Koch et al., 2001, unpublished data). We want to calculate the position of the fork and study the amount of force necessary to separate the DNA strands.

A

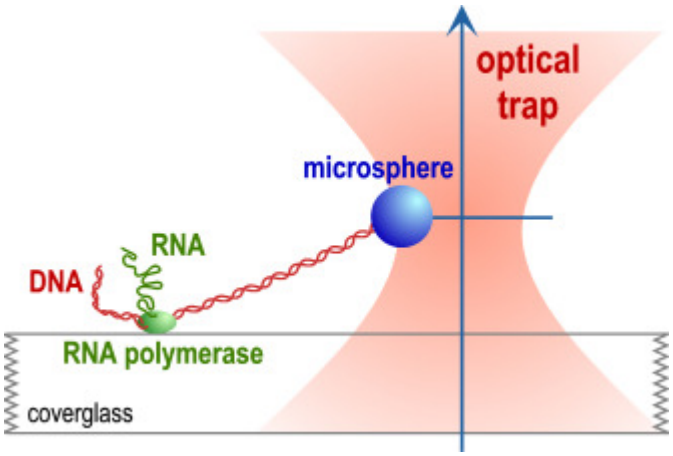
optical
trap
microsphere
RNA
DNA
RNA polymerase
coverglass

B

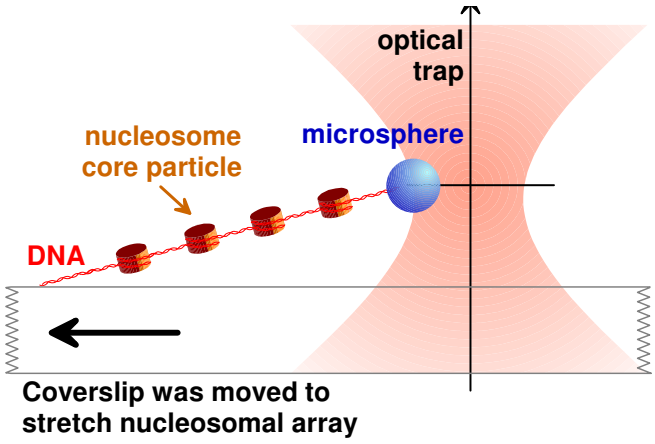
optical
trap
nucleosome
core particle
microsphere
DNA
Coverslip was moved to
stretch nucleosomal array

C

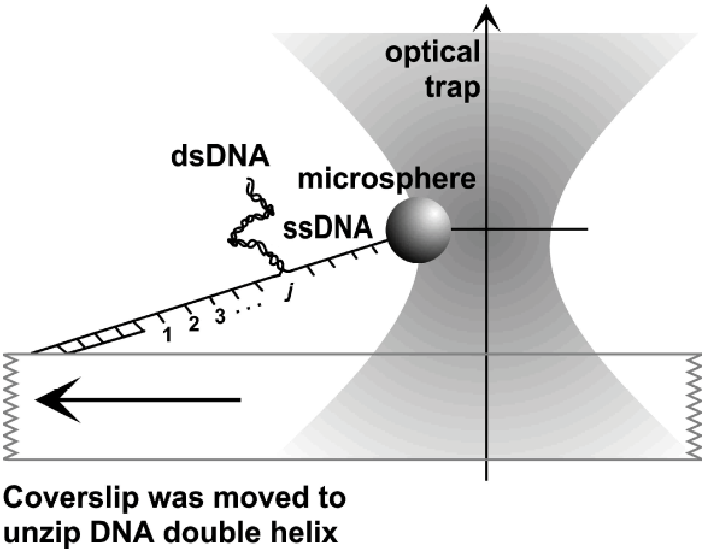
optical
trap
dsDNA
microsphere
ssDNA
1 2 3 . . . j
Coverslip was moved to
unzip DNA double helix

2. BACKGROUND: OPTICAL TWEEZERS

Optical tweezers trap small dielectric particles in the focus of a laser. For a review, please see Svoboda and Block, 1994. At the focus, the electric field intensity gradient exerts a force on induced dipoles within the dielectric

$$F = -\nabla U \propto -\nabla(-p \cdot E) = \nabla(\alpha E \cdot E) = \alpha \nabla(E^2)$$

where F is the force on each dipole, U is the potential energy, p is the induced dipole moment, E is the electric field, α is the relative polarizability. The square E^2 of the electric field is proportional to the light intensity. For a laser beam with a gaussian intensity profile,

$$\text{Intensity} \propto \exp(-r^2) \approx 1 - r^2 + O(r^4) \text{ (for small } r)$$
$$F_r \propto \frac{\partial}{\partial r} \text{Intensity} = -k \cdot r$$

where r is the distance from the beam axis and k is a constant, the optical trap is to first order a linear spring. The spring stiffness depends on the laser power, the size of the bead or particle, the characteristics of the dielectric, and the degree of focus.

The trap center is not necessarily at the beam waist or focus — which would be the location of the largest intensity gradient. The laser beam contributes a scattering force, which pushes the trap center away from the beam waist.

3. EXPERIMENTAL APPARATUS

Our optical setup is designed to bring a 1064-nm continuous-wave laser (Spectra-Physics) beam to a diffraction-limited spot near the focus of a microscope objective (Nikon 100× oil-immersion plan-Apochromat with NA=1.4). We modulate the intensity of the laser beam before it enters the microscope by using an acousto-optic deflector (AOD, Neos). We trap streptavidin-coated polystyrene (index of refraction n=1.57 (Svoboda and Block, 1994; Osswald and Menges, 1995) beads (0.48-µm diameter from Bangs Laboratories) suspended in water (n=1.33) in homemade sample chambers. We mount the sample chambers on an internally feedback-controlled piezo translator microscope stage (Physik Instrumente). Bead position relative to the trap center is measured by the deflection of the the laser beam; we detect the deflections with an infrared-sensitive quadrant photodiode (Hamamatsu S5981). The position detection is performed by an analog amplifier (On Trak OT311) that measures the currents q from the four quadrants of the photodiode and produces normalized position signals and a sum signal:

$$X = \frac{q1 - q2 - q3 + q4}{q1 + q2 + q3 + q4} \qquad Y = \frac{q1 + q2 - q3 - q4}{q1 + q2 + q3 + q4} \qquad Sum = q1 + q2 + q3 + q4$$

which we calibrate to discover bead position relative to the trap. We use a low-pass filter (Krohn-Hite) at 5 kHz to prevent aliasing within our measurements due to the data acquisition device's 13–20 kHz sample rate (National Instruments PCI-6052E). We use a computer to acquire position data about the trapped bead and to control the AOD and piezo stage. We can also use a video camera to observe the action in the microscope.

3.1 Design and Building of the Optical Tweezers

Here are some design considerations:

- We want to modulate the laser intensity with the AOD, and to control the cover glass position with a piezo stage.
- We need to have manual control of the trap position. We accomplish this by inserting a telescope into the setup where the lens earlier in the beam path is at an image plane equivalent to the microscope objective's back focal plane (Visscher et al., 1996). The telescope must be within reach of the microscope user.
- We want the trap to have as large an intensity gradient as possible. We accomplish this by having the beam overfill the back aperture of the objective (Svoboda and Block, 1994), by expanding the beam after it exits the AOD. We also want a compact setup.
- We want the position detector to measure the relative motion of the trapped bead within the trap, not the absolute position of the trap itself. We accomplish this by placing the quadrant photodiode position detector at a plane equivalent to the back focal plane of the objective (shown in Figure 2) (Visscher et al., 1996). When a bead in the sample plane changes the beam angle, the position detector receives a change in the beam position; a change in beam position in the sample plane changes only the beam angle at the position detector.

In the design of the optical tweezers setup, it is important to calculate the positions of all the optical elements and their cumulative effects on the laser beam. We calculated beam waists using formulas given by Sidney A. Self (1983) and expected image positions using ordinary ray-optics formulas. To facilitate this procedure, I created a set of software subroutines that allowed me to write computer programs whose

structure paralleled the optical setup. For example, given the characteristics of a gaussian beam (wavelength, waist position, and waist radius) and a lens (effective focal length and position), the lens subroutine computes the expected characteristics of the beam after it passes through the lens. Using these subroutines, I designed the optical setup by programming a daisy chain of subroutines representing optical elements in the same order that the beam path would later take.

The schematic of the optical tweezers setup appears in Figure 2.

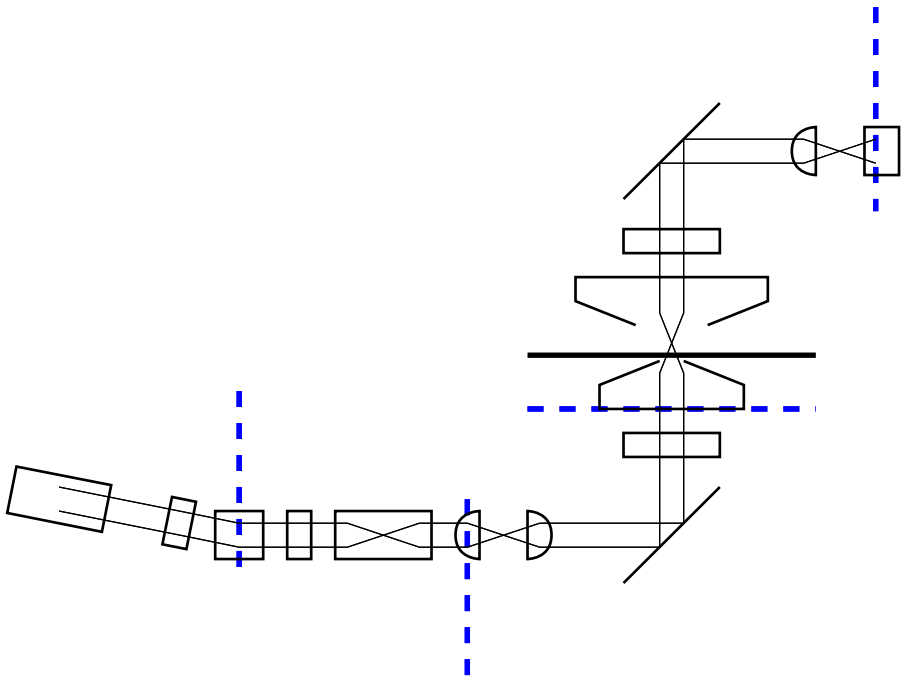

Figure 2 Schematic for optical tweezers apparatus shows laser beam path, relative locations of optical elements, and equivalent image planes.

3.2 Data Acquisition Software

The experimental setup enables a computer to acquire data while manipulating the optical trap stiffness and piezo stage position. In Professor Wang's laboratory, all of

the current experiments which use optical tweezers require observations of the dynamic behavior of a system, including its responses to predefined sets of changing conditions. I wrote a software interpreter that enables accommodates versatile experimental conditions

- powerful enough that advanced users may specify the action of any computer-controlled part of the experimental setup,
- simple enough that every lab member can learn to use it to manipulate the optical tweezers setup without performing any low-level programming, and
- versatile enough to collect data for all experiments that use the optical tweezers setup.

We use the computer to perform Proportional-Integral-Derivative feedback control in two different modes, which were both implemented by Steven J. Koch:

- In the force clamp, the computer holds the trap intensity constant while modulating the piezo stage position to maintain the bead at some particular displacement from the trap center. This is the mode most often used in the experiment shown in Figure 1-A (RNA polymerase) to follow the motion of the enzyme.
- In the velocity clamp, the computer moves the piezo stage at a constant speed while modulating the optical trap intensity to maintain the bead within some fixed displacement from the trap center. If the piezo stage begins to pull a tethered bead out of the trap, the trap stiffness will increase in an attempt to hold the bead. This is the mode most often used in the experiments shown in Figure 1-B to disrupt nucleosomes and in Figure 1-C to unzip DNA.

Other implementations of those feedback modes and even other feedback modes (Koch et al., 2001, unpublished data) are possible, but the above two have been used

most often (Brower-Toland et al., 2002). The software feedback controller allows the experimenter to modify the feedback parameters easily. The interpreter allows the experimenter to design any sequence of feedback control and data acquisition modules and specify conditions for proceeding from one mode to the next. Combined in the data acquisition program, these features provide flexibility that would be difficult to match in a hardware feedback implementation.

4. CALIBRATION

To perform accurate measurements with optical tweezers, it is necessary to calibrate two parameters: stiffness, which measures the force that it exerts on trapped beads, and sensitivity, which measures the relative position of beads within the trap.

4.1 Calibration of Trap Stiffness

The stiffness of the trap is proportional to the corner frequency of the overdamped trapped free bead's Brownian motion. Alla Shundrovsky (2001, unpublished data) measured the stiffness of the trap.

4.1.1 Background

We assume that the trap exerts a linear spring force on the bead. The one-dimensional equation of motion for a trapped bead is that of a damped driven oscillator

$$m\ddot{x} = -\beta\dot{x} - kx + \mathrm{f}(t)$$

where x is the position of the bead, m is the mass of the bead, $\beta = 6\pi\eta a$ is the Stokes drag coefficient for a sphere of radius a in a fluid of viscosity η, k is the optical trap stiffness along the x-axis, and f(t) is the Brownian forcing term, whose power spectrum is white (constant with respect to frequency). We use the Stokes expression because, as with Smith et al. (1992), the Reynolds numbers in the experiment are no greater than 10^{-2}. We convert the equation to its power spectrum representation

$$\left(m\omega^2 + k\right)^2 \left|\mathrm{X}(\omega)\right|^2 + \beta^2\omega^2\left|\mathrm{X}(\omega)\right|^2 = \left|\mathrm{F}(\omega)\right|^2 = B$$

where X(ω) is the Fourier transform of the position signal $x(t)$, F(ω) is the Fourier transform of the driving term f(t), and B is a c onstant. Our trapped beads are overdamped: far from surfaces, the viscosity of water η is

1 cP = 10^{-3} kg m^{-1} s^{-1} = 10^{-6} pN s nm^{-1} μm^{-1}. The radius a of the bead is 0.24 μm

(Wang, 2001, unpublished data).* Its Stokes drag coefficient β is about 4.5×10^{-6} pN s nm^{-1}, but its mass m is only 6×10^{-14} g = 6×10^{-14} pN s^2 nm^{-1}. Since the mass term is insignificant in the frequency regime of our experiment ($\omega < 10^5$ rad s^{-1}), we ignore it. Then the power spectrum for the bead's motion is

Equation 1: $$\left|X(\omega)\right|^2 \approx \frac{B}{\beta^2\omega^2 + k^2}$$

which has a Lorentzian roll-off with corner frequency $\omega_c = k/\beta$.

4.1.2 Method

This calibration requires free, untethered beads. We make samples with a dilute suspension of the beads in deionized water, and turn on the laser to trap a single bead. To calculate the force that the trap exerts on the bead, we need to know the trap stiffness k. We measure the power spectrum of the position signal of a trapped bead and fit each spectrum to Equation 1 to find the cutoff frequency $\omega_c = k/\beta$, as shown in Figure 3. We measure the dependence of this cutoff frequency on two quantities:

- laser power, which we assume directly affects the trap stiffness k, and
- trap height — the distance from the center of the trap to the surface of the cover glass — which affects the viscosity η of the surrounding water (Svoboda and Block, 1994) and may affect the trap stiffness k by changing the amount of aberration.

* This fails to account for the possible presence of a charged ionic layer when the beads are in solution.

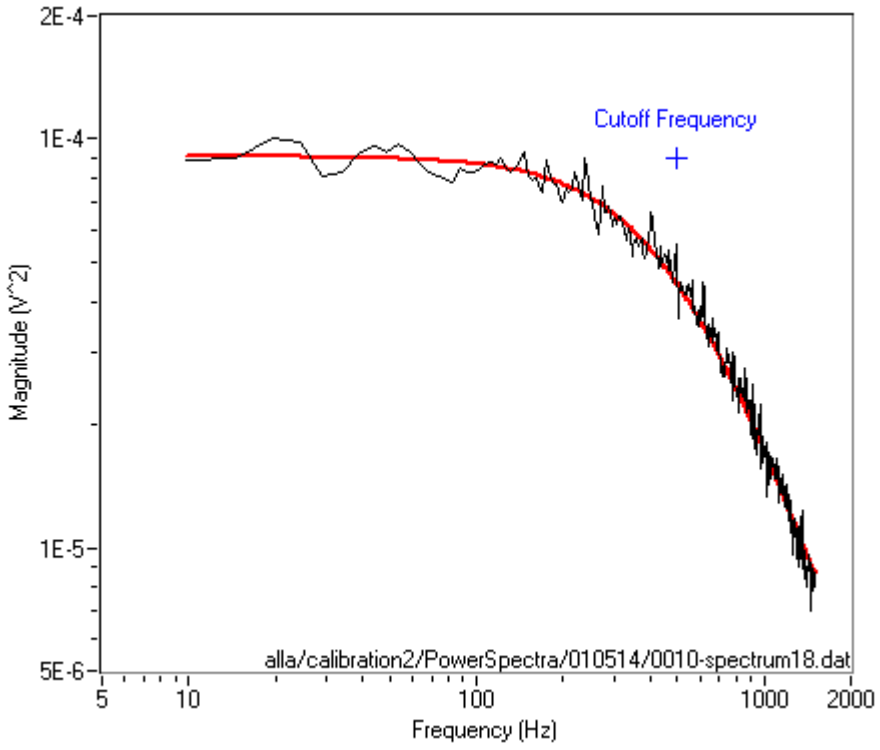

Figure 3 Power spectrum for 1-dimensional motion of trapped free bead shows a Lorentzian profile. We fit the power spectrum to find the cutoff frequency and the trap stiffness. The thin curve shows the raw data; the thick curve is the fit.

4.1.3 Results

We calibrate the stiffness of the optical tweezers using corner frequencies between 300 and 1500 Hz. Below 300 Hz, mechanical equipment noise interferes with the data; above 1500 Hz, the On-Trak OT311 amplifier introduces a single-pole cutoff which makes fitting inaccurate (unpublished data, 2000). For our beads, the corner frequency reaches 1500 Hz at a laser power of about 100 mW. In Figure 3, the laser power was about 26 mW.

Alla Shundrovsky found that the trap stiffness k in the X direction was 9.546×10^{-5} pN nm^{-1} (mV Sum)$^{-1}$, or 1.123×10^{-5} pN nm^{-1} (mW laser)$^{-1}$ (2001, unpublished data). We

calculate the force exerted on the bead by multiplying the trap stiffness k by the distance X_{bead} from the bead to the trap center, which we calibrate in the next section.

4.2 Calibration of Position Detector Sensitivity

4.2.1 Method

To calibrate the position detector, we affix beads to the surface of the sample chamber and use the piezo stage to move single beads through the laser beam. (Steven J. Koch (2000, unpublished data) found that the specifications given by the data acquisition board and piezo stage and microscope and video camera manufacturers appear to be consistent.) The position detector signal along the axis parallel to the bead motion (x) appears in Figure 4.

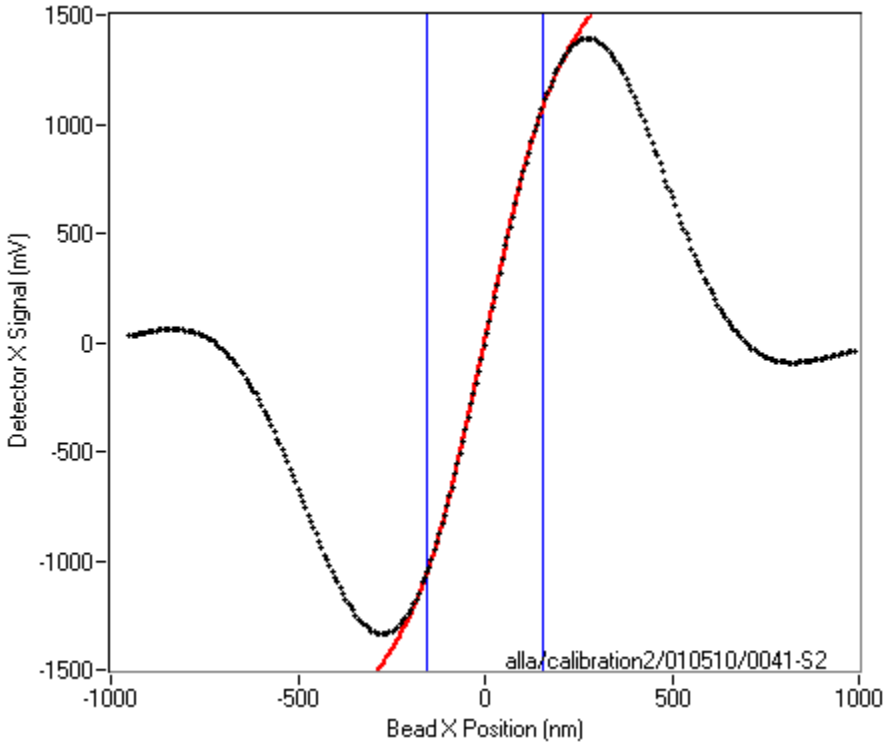

Figure 4 Detector signal due to movement of a single bead through the optical trap (shown as + points) has a usable region of 300 nm (delimited by the vertical lines), which we fit to an odd polynomial function (shown as solid curve).

We use only the center 300-nm range and fit it to an odd polynomial function. The sensitivity (the slope of the boxed curve in Figure 4) depends on the position of the bead within the trap. Alla Shundrovsky (2001, unpublished data) measured this variation with respect to the axis of the laser beam (z); her results appear in Figure 5.

4.2.2 Variation of Sensitivity with Relative Bead Position

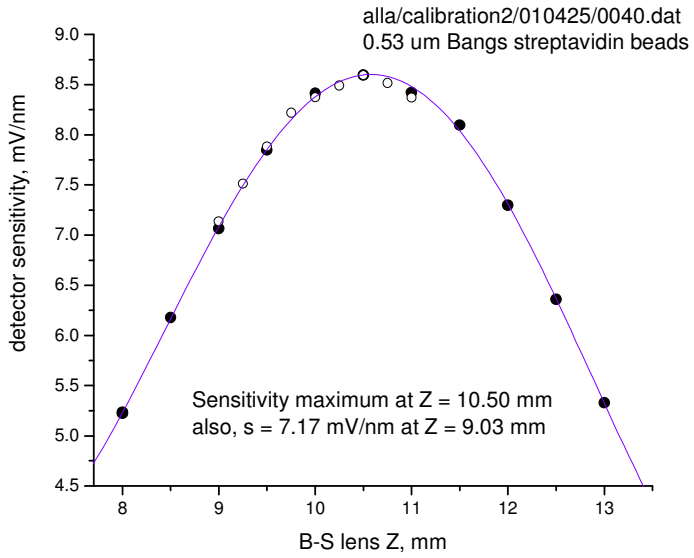

Figure 5 Position detector sensitivity depends on relative height of bead center and beam waist. The vertical axis is the slope of the fit curve in Figure 4. The horizontal axis, labelled "B-S lens Z, mm", is the micrometer setting for the beam-steering lens in Figure 2 (lens L7 in Figure 13). Figure courtesy of Alla Shundrovsky.

When we use the optical tweezers setup to stretch DNA tethers, the tether pulls the bead down, away from the trap center, toward the beam waist. We expect that the position detection will be more sensitive when the bead is closer to the beam waist, because it will then occupy a greater fraction of the beam cross-section. The sensitivity can increase by about 20%, which is significant when using an average displacement of 80 nm from the bead to the trap center.

4.2.3 Calculation of Sensitivity at Trap Center

It is also possible to calculate the sensitivity *s* of the position detector at the trap center by applying the virial (Goldstein, 1980) and equipartition (Pathria, 1996) theorems to describe the energy of the trapped bead and knowing the trap stiffness *k*, the position detector signal (voltage) variance $\langle v^2 \rangle$, and the temperature, as follows:

$$\tfrac{1}{2} k \langle x^2 \rangle = \tfrac{1}{2} k_B T \qquad \Rightarrow \qquad \langle x^2 \rangle = k_B T / k$$

$$s = v / x = \sqrt{\langle v^2 \rangle / \langle x^2 \rangle} = \sqrt{k \langle v^2 \rangle / k_B T}$$

We must assume that $\langle x \rangle = \langle v \rangle = 0$, which is true for trapped free beads.

5. BACKGROUND: DNA

5.1 Structure

Double-stranded deoxyribonucleic acid (dsDNA) consists of two helical linear polymers. Figure 6 shows the molecular structure of a typical DNA fragment. The polymeric units are nucleotides. Each nucleotide consists of a base (adenine, guanine, cytosine, thymine), a sugar, and a phosphate group. The sequence of bases contains genetic information; the sugar and phosphate form the backbone of the polymer.

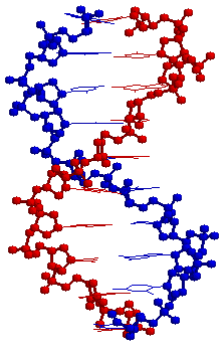

Figure 6 dsDNA consists of two helical linear polymers. The nucleotide bases are shown as thin wireframes; the sugar and phosphate backbones are shown as ball-and-stick structures. Structure drawn from coordinates in file 1dcv.pdb (Eichman et al., 2000).

The two strands are oriented in opposite directions, which are called "5´-to-3´" and "3´-to-5´", depending on the number of the sugar's carbon atom attached to the next phosphate. The bases occur in Watson-Crick pairs: an adenine on one strand with thymine on the other strand; guanine on one strand with cytosine on the other. X-ray diffraction data have shown that the base pairs occur at a spacing of 0.34 nm in DNA crystals.

5.2 Elasticity

In the low-force region, the molecule is slack; the molecule becomes taut as the extension *LDNA* (nm) increases to the contour length of the tether. Michelle D. Wang (1997) showed that this empirical DNA elasticity relationship is fit by the modified Marko-Siggia wormlike chain expression:

Equation 2: $$F = \left(\frac{k_B T}{L_P}\right)\left(\frac{1}{4(1 - x/L_o + F/K_o)^2} - \frac{1}{4} + \frac{x}{L_o} - \frac{F}{K_o}\right)$$

where F is the tension in the tether, K_o is the stretch modulus of DNA, $k_B T$ is the thermal energy, L_P is the persistence length of DNA, x is the extension (L_{DNA}) of the DNA tether, and L_o is the contour length of the tether. The stretch modulus K_o and persistence length L_P parameters are material characteristics of the DNA and the surrounding chemical environment (Wang et al., 1997; Baumann et al., 1997; Baumann et al., 2000): they may depend on the sequence or ratio of the nucleotides, but not on the length of the molecule.

6. EXPERIMENTAL CONFIGURATION

6.1 Methods

Since the DNA molecule is flexible, we must extend it to measure its length. We attach one end of the molecule to a movable cover glass and the other end to a bead held in an optical trap. We stretch the molecule by moving the cover glass while monitoring the tension in the DNA tether (equal to the force exerted by the optical trap). We fit the resulting force-extension characteristic to calculate the tether length.

Stretching experiments were performed at 22 ^{o}C in buffer containing 10 mM Tris HCl (pH 8.0), 1 mM Na_2EDTA, 100 mM NaCl, and 0.02% (v/v) Tween-20. The DNA fragment was labeled at one end with biotin, and at the other end with digoxigenin (Roche) (see "Appendix A: Preparation of the DNA " for more detail). Prior to stretching, one end of each DNA fragment was attached to the surface of an anti-digoxigenin (Roche) –coated microscope cover glass. A 0.48-μm diameter streptavidin-coated polystyrene bead (Bangs) was then attached to the free end of each tethered array. Biotin-streptavidin and the digoxigenin–anti-digoxigenin linkages can withstand more than 60 pN of force over the period of our experiments.

6.2 Geometry of DNA Length Calculation

Since our detection and controls are only along the horizontal direction whereas the DNA tether is at an angle relative to the horizontal, we determine the length L_{DNA} of the DNA molecule by considering the geometry of the experimental configuration, which appears in. Figure 7. Below, I discuss each parameter in detail.

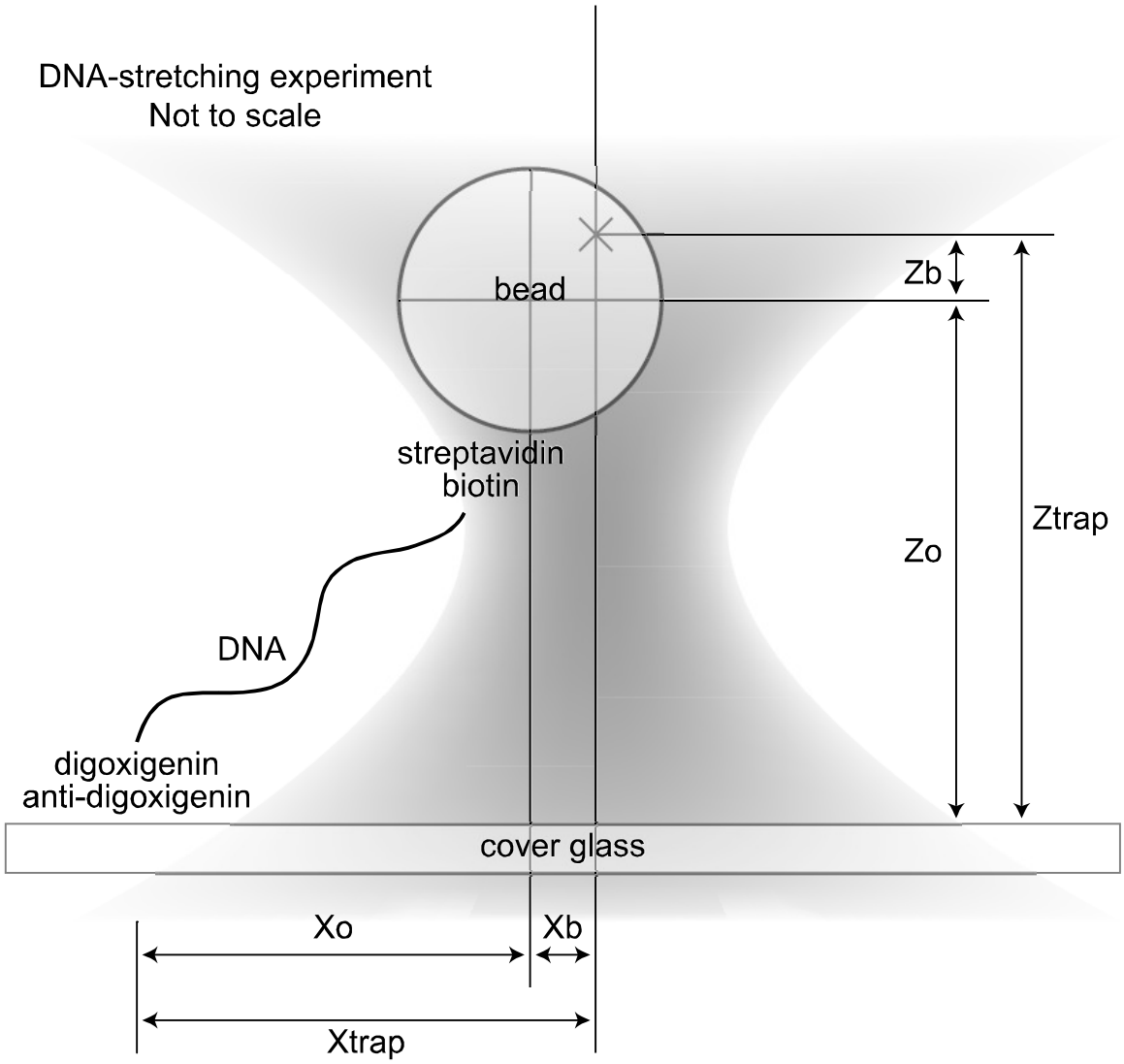

Figure 7 The experimental configuration contains many geometrical parameters that must be considered when calculating the length of the DNA

6.2.1 X_{bead}

X_{bead} is the absolute distance from the axis of the trap to the center of the bead. We measure this with the position detector. As mentioned earlier, the detector sensitivity depends on the distance Z_{bead} from the bead to the trap center. We first calculate X_{bead} at $Z_{bead} = 0$, then calculate the resulting Z_{bead}, and iterate.

6.2.2 X_{trap}

X_{trap} is the absolute distance (parallel to the direction of motion of the piezo stage) from the axis of the trap to the tether anchor point. We measure this by stretching the tether from side to side after assuming that the optical trap is cylindrically symmetric. The position detector signal for the tether center determination process, shown in Figure 8, contains a middle region where the DNA tether, slack, allows the bead to dwell at the trap center.

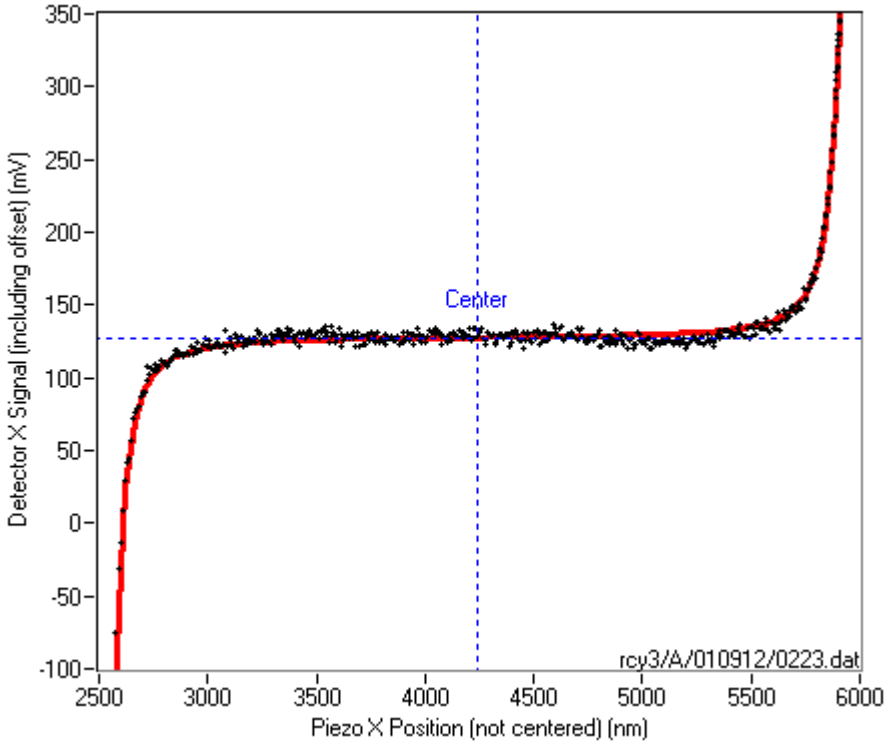

Figure 8 Symmetric position detector signal (shown as + points) for a tethered bead pulled from one side of the trap to the other defines a unique center point. Data from file Aatte/rcy3/A/010912 DNA 4400 bp/0223.dat (000).

We define the piezo position for the symmetry point of the position detector signal to be the zero point of X_{trap}.

6.2.3 $X_o = X_{trap} - X_{bead}$

We assume that the quadrant photodiode position detector is aligned with the piezo stage's direction of motion.

6.2.4 Z_{trap}

Z_{trap} is the Z distance (height) of the trap center above the cover glass surface, which we hold constant in our experiments. In the course of calibrating the optical trap stiffness and position sensitivity, Alla Shundrovsky determined the dependence of Z_{trap} on the beam-steering telescope lens position through two independent methods:

- Faxen's law gives the fluid viscosity as a function of the ratio of the distance from the cover glass surface to the radius of the bead (Svoboda and Block, 1994). By fitting the trapped free bead's corner frequency as a function of the beam-steering telescope lens position to this relation, we can determine the height of the trap.
- The stiffness calibration also allows us to find the sensitivity of the position detector at the trap center (see p. 14). By comparing this sensitivity to the data in Figure 5, relating sensitivity to beam-steering telescope lens position, we can determine the effective separation of the waist and the trap in beam-steering lens position units. Finally, we must discover the conversion between the beam-steering lens position and the beam waist position: we affix beads of various known sizes to the cover glass and find the beam-steering lens position of greatest sensitivity, which should occur at the coincidence of the beam waist with each bead center. This last step assumes that the portion of the beam path in the polystyrene bead material is equivalent to the same distance in water, which is a good approximation for beads smaller than 0.5 μm in diameter.

6.2.5 Z_{bead}

Z_{bead} is the axial displacement of the bead from the trap center, and is determined using the following relation (Wang et al., 1997):

Equation 3: $$Z_{\text{bead}} = \frac{Z_{\text{trap}}}{\left(\frac{k_z}{k_x}\right)\left(\frac{X_o}{X_{\text{bead}}}\right)+1}$$

By measuring the corner frequencies of the position detector X and Sum (which can sometimes indicate Z_{bead}) signals, Steven J. Koch (2001, unpublished data) determined the ratio of stiffnesses k_x/k_z to be 4.5.

After using Equation 3 to calculate Z_{bead}, we iterate to correct the sensitivity used to calculate X_{bead}. This process usually settles after about 5 to 10 iterations.

7. RESULTS AND DISCUSSION

7.1 Strategy

I want to determine the accuracy and precision of the optical tweezers setup. To address accuracy, I stretched two populations of tethers: one with 4400-bp DNA fragments and one with 1155-bp fragments. To address precision, I repeatedly stretched some of the 4400-bp tethers. In both cases, I converted the stretch data and fit them to the modified Marko-Siggia wormlike chain expression.

7.2 Long tether stretch results

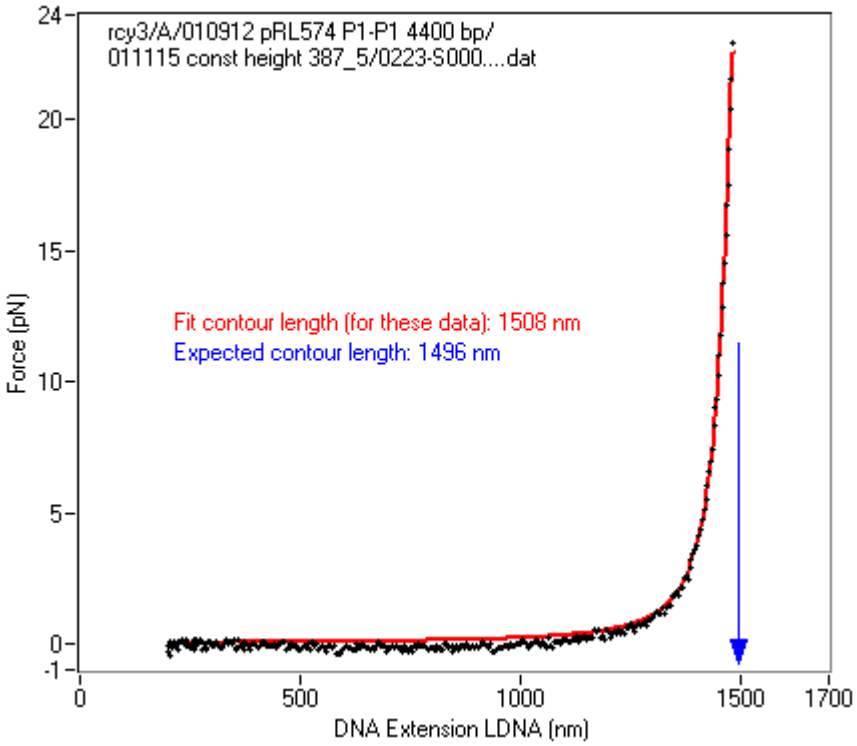

Figure 9 Force-extension data for double-stranded DNA (shown as + points) are fit by the modified Marko-Siggia wormlike chain expression (shown as solid curve).

I measured force-extension curve of single molecules of DNA of 4400 bp. An example is shown in Figure 9. Data are well-fit by the modified Marko-Siggia expression shown in Equation 2.

I stretched 24 DNA molecules. Figure 10 shows the large distributions of fit parameters for the force-extension curves. For example, the standard deviation of tether length from different molecules is 72 nm. I conducted several experiments to investigate the sources that contribute to the spread. Below I will only use tether length for error diagnosis since it is relatively insensitive to fitting algorithm.

7.3 Long tether stretch discussion

7.3.1 Determination of the precision of the instrument.

The precision of the instrument is determined by repetitively stretching the same DNA molecule and computing the standard deviation in tether length measured from the repeated stretches. I did this four times for one tether and three times for another. The standard deviations (in nm) were 11.4, 9.6, 11.9, 6.9, 9.2, 4.7, 2.7; the average standard deviation is 8.1 nm. This is much smaller than the overall spread of 72 nm as shown in Figure 10. Instrument imprecision could result from electronic and instrument drift.

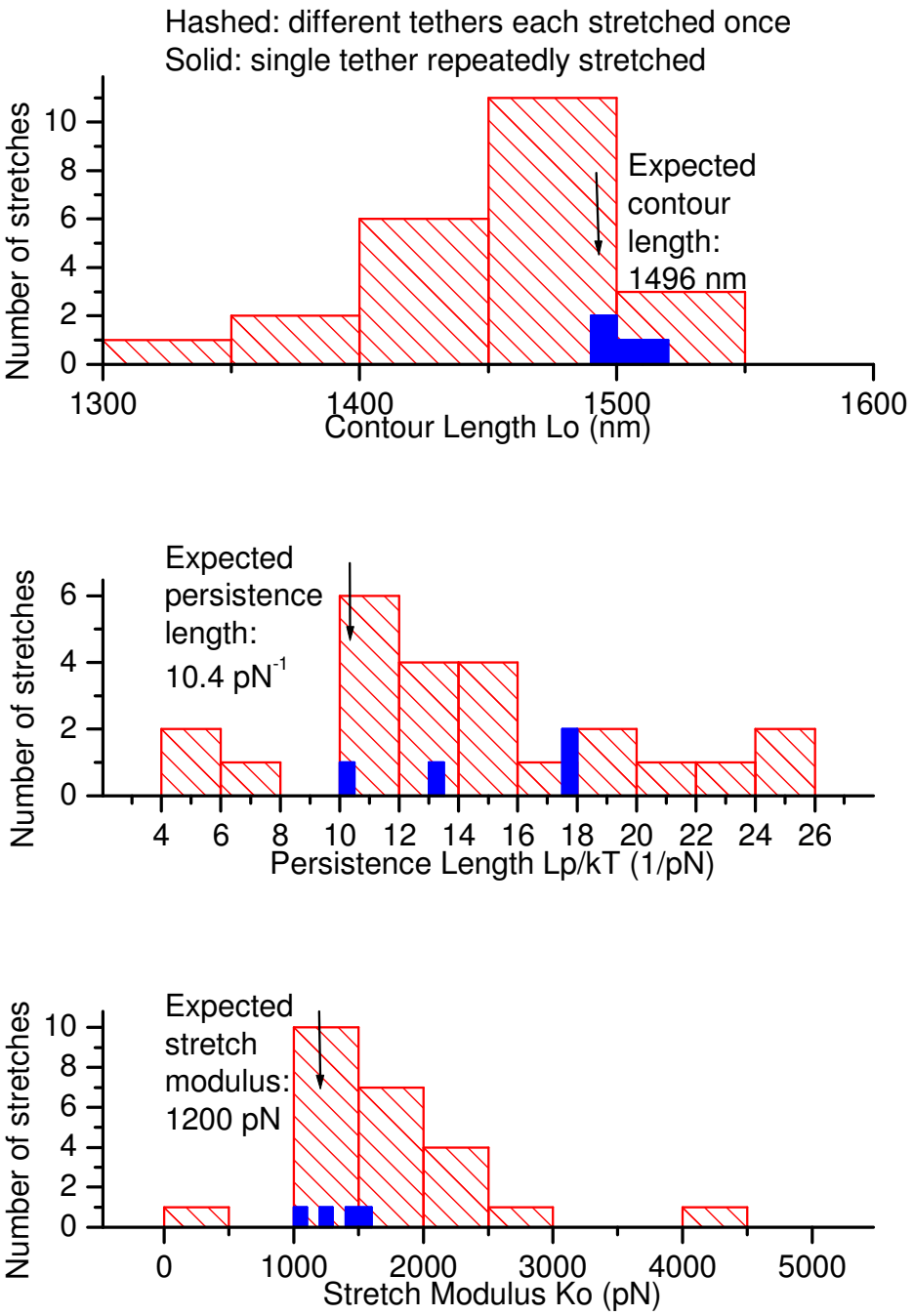

Figure 10 Distribution of fit parameters for 4400-bp DNA tethers is broader than that for a single tether stretched multiple times. Hashed bars ( ) indicate the distribution of fit parameters for only the first stretch attempt on each of 24 4400-bp DNA tethers. Solid bars ( ) show the fit parameters for the multiple stretches (after recentering and refocusing the instrument between each stretch attempt) for a single 4400-bp DNA tether.

7.3.2 Determination of human errors in trap positioning

DNA molecules are assumed to be stretched along the X direction (i.e., at Y=0). However, unlike the determination of the center along the X axis, the centering of the trap in the Y-direction is performed manually. The offset in Y will cause the data to underestimate the tether length. The error resulting from this problem is investigated by repetitive measurements of the tether length from the same molecule after manually repositioning. The results of this study is shown in Figure 10 (solid bars). The standard deviation is 13.5 nm. To confirm that this error is consistent with the trap positioning error in Y, we would like to estimate the Y error directly. However, our instrument did not permit us to stretch along Y, which would have allowed us select the Y zero point correctly. Instead, we use the trap X positioning error to estimate that of the Y since we center the trap along X and Y in a similar fashion. The tether anchor positions for two tethers each stretched multiple times appear in Table 1.

Table 1 Tether center positions for repeatedly-stretched long tethers reveal a trend in successive stretch attempts and the precision of positioning the apparatus on a tether.

Stretch attempt (tether in file 208)	Center (nm)	Stretch attempt (tether in file 213)	Center (nm)
0 (original)	4240	0 (original)	3630
1	4248	1	3631
2	4261	2	3666
3 (recentered)	4663	3 (recentered)	3583
4	4682	4	(failed)
5 (recentered)	4116	5	3601
6	4131	6 (recentered)	3545
7	4119	7	3562
8 (recentered)	4595	8	3543

When tethers are re-stretched without re-centering (stretch attempts with no parenthetical comment), successive center positions appear to have translated toward higher values. This trend is measured and discussed on page 37. When I re-centered

the apparatus on the tethers (before acquiring data for stretch attempts marked with "(recentered)"), the human imprecision in positioning the expected position of the laser trap on the tether point had a standard deviation of 231 nm in file 208 and 35 nm in file 213. For a 1496-nm DNA tether, a 231-nm centering error in Y would reduce the apparent length by 18 nm

7.3.3 Determination of the sample quality over time.

Experiments from (1) and (2) show that the instrument error and the human trap positioning error are not the major sources of error for tether length determination. I discovered that a major source of error is the degradation of sample quality over time. Figure 11 shows the measurement of tether length as a function of sample age.

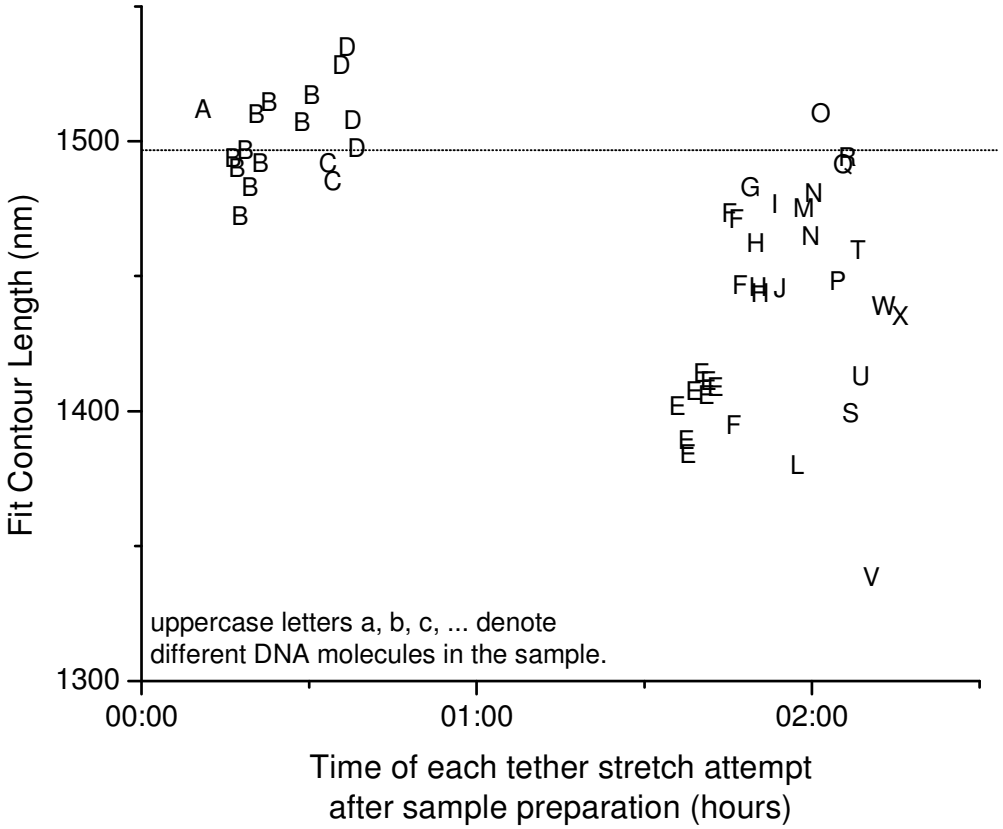

Figure 11 Tether contour length uniformity degrades with time, while the precision of tether length measurement for single tethers remains unchanged. The expected contour length for all tethers shown here is 1496 nm.

There is a systematic decrease in average tether length over time with an increase in the tether length distribution. The cause of this degradation is unknown, but it may be due to nonspecific sticking of the DNA to the bead or to the cover glass. The clustering of fit contour lengths for repeated stretches of single tethers suggests that the precision of the instrument was unchanged.

7.4 Short tether stretch results

I repeated the above experiment with 1155-bp DNA fragments instead of the 4400-bp DNA fragments. The histogram of the fit parameters appears in Figure 12. None of the fit parameters was close to its expected value. Uncertainties in both the Y direction and the Z direction affected the length determination for short tethers more strongly than for long tethers. For a 393-nm DNA tether, a 231-nm Y-axis centering error would reduce the apparent length by 75 nm, which could explain much of the deviation from the expected value.

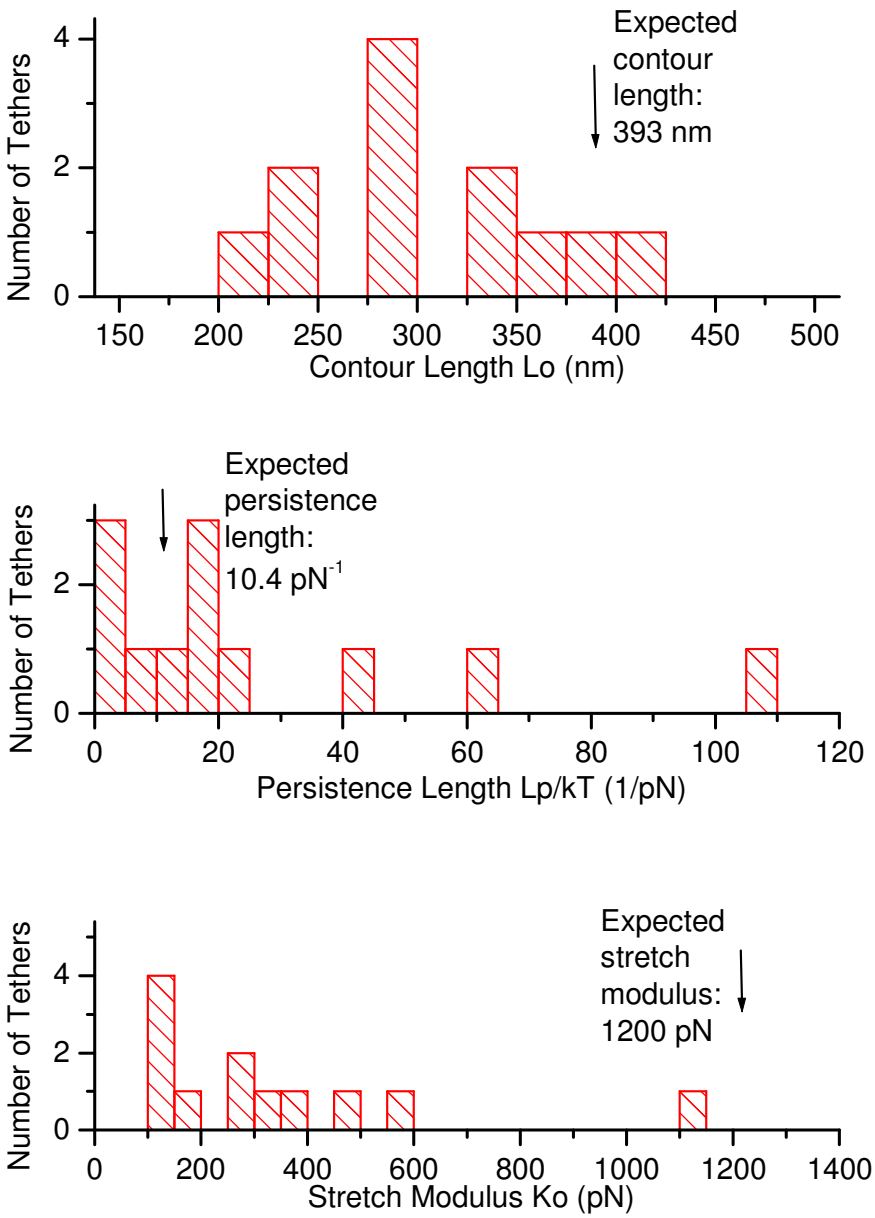

Figure 12 Distribution of fit parameters for short tethers differs from the expected values, showing that the present data collection and conversion method is unsuitable for experiments on short DNA tether constructs. This graph shows only the first stretch attempt on each tether; the data are from files 241–254, 257.

7.5 Summary of force-extension fit parameters

Table 2 summarizes the fit parameters for repeated stretches of a single long tether, the first stretch attempts for all long tethers, the first stretch attempts for all short tethers, and previously published results.

Table 2 Summary of fit parameters for DNA tether stretch data.

Category	Contour Length (nm) mean ± SE (n) [Expected Length]	Persistence Length L_P/k_BT (/pN) mean ± SE (n)	Stretch Modulus (pN) mean ± SE (n)
Repeated same 4400-bp tether (solid bars in Figure 10)	1502±4 (4) [1496]	14.7±1.8 (4)	1316±104 (4)
Different 4400-bp tethers (hashed bars in Figure 10)	1446±15 (24) [1496]	14.2±1.1 (24)	1710±160 (24)
Different 1155-bp tethers (shown in Figure 12)	307±19 (12) [393]	25.6±9.1 (12)	347±82 (12)
Previous results		*(with slightly different buffers)*	
Wang et al., 1997	674±6 (5) [661]	10.17±0.58 (4)	1010±99 (5)
Wang et al., 1997	1348±6 (5) [1328]	10.41±0.31 (5)	1205±87 (5)
Wang et al., 1997	1343±5 (10) [1322]	11.45±0.24 (14)	1008±38 (10)
Smith et al., 1996	16400 [16393]	15.76	
Baumann et al., 2000	16,745±82.4 (3) [16490]	13.07±0.80 (3)	

We compare the fit contour lengths to the expected lengths of each category of DNA tethers and find that only the repeated stretches of the new 4400-bp DNA tether is stretched and converted correctly. The force-extension data for both the entire group of (new and old) 4400-bp tethers and the 1155-bp tethers agree less well the expected contour length of the DNA.

The persistence length and stretch moduli parameters are more subtle. Fitting the former requires good low-force data. The latter needs good high-force data. We compare the fit persistence lengths and stretch moduli to those reported by M. D. Wang (1997). In every case, the fit persistence length is greater than that

previously reported. Only the new 4400-bp tether has a stretch modulus within error of the previous result; the average for all the other 4400-bp tethers is too high and the average for the 1155-bp tethers is too low.

8. CONCLUSIONS

The standards that we use to calibrate the optical tweezers setup do not depend on DNA. We check the calibration by stretching DNA molecules and comparing the fit elasticity parameters to previously published data.

Due to its speed, noninvasive (except perhaps local heating) nature, and convenience in the manipulation of microscopic objects, the optical trap is an excellent tool for single-molecule studies — but only those that can accommodate its limitations, which in our setup include:

- imprecision (200 nm) in the initial manual positioning of tethers;
- a useful lifetime of one hour or less for single samples of DNA tethers;
- inaccuracy in the stretching or geometry conversion for short (400-nm or less) tethers.

APPENDIX A: PREPARATION OF THE DNA FRAGMENTS

I produced DNA through 33 cycles of the polymerase chain reaction (PCR) (Kramer et al., 1994) on pRL574 plasmid DNA with two pairs of primers. Primer P1-dig-F-pRL574 (Synthegen) contains a digoxigenin (Roche) label at its 5´ end; primers P1-bio-R-pRL574 (Synthegen) and P13-bio-R-pRL574 (Invitrogen) each contain a biotin label at its respective 5´ end. The PCR product due to primers P1-dig-F-pRL574 and P1-bio-R-pRL574 is a 4400-bp dsDNA segment. The PCR product due to primers P1-dig-F-pRL574 and P13-bio-R-pRL574 is a 1155-bp dsDNA segment. Both PCR products were purified separately by using QiaQuick spin columns (Qiagen, Inc.).

APPENDIX B: OPTICAL SETUP

The layout of the optical tweezers setup appears in Figure 13. During the alignment process, we checked the imaging calculation by placing a CCD camera's image detector plane near the penultimate equivalent back focal plane (later the position of the manual beam-steering lens — L7 in Figure 13) before the microscope objective. We recorded images of the dust and scratches on the beam-entry and -exit surfaces of the AODs and the other manual beam-steering lens (lens L5 in Figure 13).

Figure 13 The layout (to scale) for the optical tweezers apparatus consists of a laser source (top center) and optical elements placed to bring the beam to the microscope (bottom left). The user sits in front of the microscope, somewhere below the bottom edge of the figure. The filled "•" dots and small "×" marks denote the optical mounts' screw positions; the large "×" marks, for reference only, represent a square grid spaced at five inches. The shaded optical elements, labeled "AOD-S", "AOD-P", "L5", and "L7", are at planes equivalent to the back focal plane of the microscope objective. The quadrant photodiode position detector (not shown in the layout) is placed after the microscope, also at a plane equivalent to the back focal plane of the microscope objective.

APPENDIX C: FUTURE WORK

Although we have characterized and calibrated the most prominent features of the optical tweezers setup, a few unresolved details remain.

Unidirectional drift problem

As mentioned in the results section (see Table 1), it appears that successive center positions appear to have been translated toward higher values. I investigated this by repeatedly moving a stuck bead through the trap. The detector signal from this experiment appears in Figure 14. I confirm that the stuck bead signal translates in the course of the experiment.

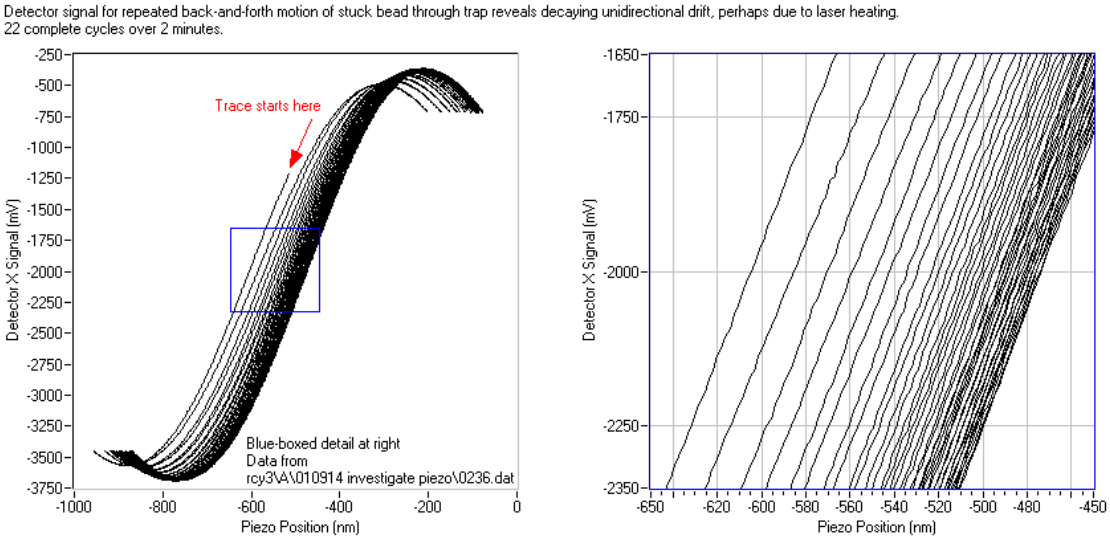

Figure 14 Repeated back-and-forth motion of stuck bead through trap (analogous to Figure 4) reveals decaying unidirectional drift —20 nm in the first 3 seconds, then 15 nm, then 10 nm.

I later showed that exposing the setup to the laser for a minute or two before attempting to take these data would reduce the amount of spurious translation observed. I failed to compensate for this spurious translation in this thesis's data, but I attempted to reduce it in two ways:

- I stretched the tethers at a high stretch rate and used data on the tether center as close in time to the final stretch as possible; and
- when stretching the short tethers, I continued to expose the setup to the laser, to maintain the apparatus in as close to a steady-state condition as possible.

Y centering

In the future, a tweezers setup that incorporates two-dimensional centering may be built. For now, a quick implementation would be to rotate the piezo stage by 90° and use the AODs to steer the trap to center in the X direction and then move the piezo stage to center in the Y direction.

Z-detection implementation

Detection of bead position along the Z axis would reduce the number of geometrical assumptions needed to convert the data.

Resolution of the Y crosstalk problem

The X-Y position detector crosstalk problem is most likely due to the displacement of the orthogonal polarizations in the trapping laser beam due to the Wollaston prisms used to produce the differential-interference contrast microscope image.

Temperature control

The viscosity of the water used to calibrate the optical trap stiffness depends on the temperature of the solution. It varies by 10% from 20°C to 25°C, which is the likely temperature range of the sample.

REFERENCES

Baumann, C. G., S. B. Smith, V. A. Bloomfield, and C. Bustamante. 1997. Ionic effects on the elasticity of single DNA molecules. *Proc. Natl. Acad. Sci. USA.* 94:6185–6190.

Baumann, C. G., V. A. Bloomfield, S. B. Smith, C. Bustamante, M. D. Wang, and S. M. Block. 2000. Stretching of Single Collapsed DNA Molecules. *Biophys. J.* 78:1965–1978.

Brower-Toland, B. D., C. L. Smith, R. C. Yeh, J. T. Lis, C. L. Peterson, and M. D. Wang. 2002. Mechanical Disruption of Individual Nucleosomes Reveals a Reversible Multistage Release of DNA. *Proc. Natl. Acad. Sci. USA.* In press.

Cluzel, P., A. Lebrun, C. Heller, R. Lavery, J. L. Viovy, D. Chatenay, F. Caron. 1996. DNA: An Extensible Molecule. *Science.* 271:792–794.

Eichman, B. F., J. M. Vargason, B. H. Mooers, and P. S. Ho. 2000. The Holliday junction in an inverted repeat DNA sequence: sequence effects on the structure of four-way junctions. *Proc. Natl. Acad. Sci. USA.* 97:3971–3976.

Goldstein, H. 1980. *Classical Mechanics.* Addison-Wesley Publishing Company, Reading, Massachusetts. pp. 82–85.

Kramer, M. F., and D. M. Coen. 1994. Enzymatic Amplification of DNA by PCR: Standard Procedures and Optimization. In Ausubel, F. M., R. Brent, R. E. Kingston, D. D. Moore, J. G. Seidman, J. A. Smith, and K. Struhl (Eds.). 1987–2000. *Current Protocols in Molecular Biology.* John Wiley & Sons, Inc. Chapter 15.1.

National Instruments. October 1994. *LabWindows®/CVI PID Control Toolkit Reference Manual.* National Instruments Corporation, Austin.

Pathria, R. K. 1996. *Statistical Mechanics.* Butterworth & Heinemann. pp. 63–65.

Sambrook, J., E. F. Fritsch, and T. Maniatis. 1989. *Molecular Cloning: A Laboratory Manual.* Cold Spring Harbor Laboratory Press, New York. Volume 3, Appendix B.

Self, S. A. 1983. Focusing of spherical Gaussian beams. *Applied Optics.* 22:658–661.

Smith, S. B., Y. Cui, and C. Bustamante. 1996. Overstretching B-DNA: The Elastic Response of Individual Double-Stranded and Single-Stranded DNA Molecules. Science. 271:795–799.

Smith, S. B., L. Finzi, and C. Bustamante. 1992. Direct Mechanical Measurements of the Elasticity of Single DNA Molecules by Using Magnetic Beads. *Science.* 258:1122–1126.

Svoboda, K., and S. M. Block. 1994. Biological Applications of Optical Forces. *Annu. Rev. Biophys. Biomol. Struct.* 23:247–285.

Visscher, K., S. P. Gross, and S. M. Block. 1996. Construction of Multiple-Beam Optical Traps with Nanometer-Resolution Position Sensing. *IEEE J. Sel. Top. Quant.* 2:1066–1076.

Wang, M. D., M. J. Schnitzer, H. Yin, R. Landick, J. Gelles, and S. M. Block. 1998. Force and velocity measured for single molecules of RNA polymerase. *Science.* 282:902–907.

Wang, M. D., H. Yin, R. Landick, J. Gelles, and S. M. Block. 1997. Stretching DNA with Optical Tweezers. *Biophys. J.* 72:1335–1346.